

Modeling and Dynamic performance of Energy Storage -Rotary Series Elastic Actuator for Lumbar Support Exoskeleton

Omar Sabah Al-Dahiree
Department of Mechanical
Engineering, Faculty of Engineering
University of Malaya
Kuala Lumpur, Malaysia
omarsmech@gmail.com

Mohammad Osman Tokhi
School of Engineering
London South Bank University
London, UK
tokhim@lsbu.ac.uk

Raja Ariffin Raja Ghazilla
Department of Mechanical
Engineering, Faculty of Engineering
University of Malaya
Kuala Lumpur, Malaysia
r_ariffin@um.edu.my

Gan Woun Yoong
Department of Mechanical
Engineering, Faculty of Engineering
University of Malaya
Kuala Lumpur, Malaysia
eddiegan91@gmail.com

Hwa Jen Yap
Department of Mechanical
Engineering, Faculty of Engineering
University of Malaya
Kuala Lumpur, Malaysia
hjjap737@um.edu.my

Abstract—The assistive exoskeletons are rapidly being developed to collaborate with humans, and the demand for the safety of human-robot interaction has become more crucial. Series elastic actuators (SEAs) have recently been developed in various fields for a variety of possible advantages, such as providing a safe human-robot interaction, reducing the impacts' effects, and increasing energy efficiency. However, achieving the good dynamic performances of SEAs is still challenging, especially fulfilling the high bandwidth with good compliance. In this rapidly growing research field, the actuation system involving the storage device combined with the rotary series elastic actuator (ES-RSEA) is being investigated to exploit the biomechanical energy while maintaining compliance features. In this article, the modeling and control design of the energy storage rotary series elastic actuator (ES-RSEA) for the lumbar support exoskeleton is proposed, and its dynamic performances are analyzed. The ES-RSEA was designed based on storing the kinetic energy during the lifting tasks and generating assistive torque while maintaining excellent compliant characteristics. The dynamic performances and characteristics of ES-RSEA are presented in terms of force sensitivity, level of compliance, transmission ratio, and bandwidth. Simulation studies indicate that the actuator can provide excellent dynamic performance through its high bandwidth (12.44 Hz) and high force sensitivity. At the same time, it shows excellent compliance and good torque transmissibility in the low-frequency range. A PID controller can achieve high torque tracking performance and good dynamic response with a root-mean-square (RMS) error of 0.1 N.m. This article demonstrates the excellent performance and characteristics of ES-RSEA to guarantee compliance and high response to prevent injury of undesired human movements.

Keywords: Exoskeleton, lumbar support, series elastic actuators (SEA), dynamic analysis, controller, modeling

1. INTRODUCTION

Lumbar spine injuries are considered the highest risk factor in industrial workplaces involving heavy lifting and manual material handling (MMH) [1]. The exoskeleton technology has been introduced as a new approach to prevent the risk of back injuries in workers while maintaining human flexibility and strength [2]. These

wearable bionic devices enable the human body to reduce the requirement of muscular effort or lumbar stress during manual material handling (MMH) [3, 4]. The assistance torque of the exoskeleton is transmitted to the human torso by placing the actuators at hip joints. The actuation system can be assorted into passive and active actuators according to the core of their assistive source. The passive actuators mostly utilized passive components such as springs, dampers, and the elastic band as an assistive source in the lumbar support exoskeleton. Since the passive actuators are not able to provide sufficient assistance to muscle activity [5], the active actuators have been developed to generate higher power assistance to the human body by using an external power source to supply the actuators. Different types of active actuators have been used in the lumbar support exoskeleton to augment the human muscle for example electric motors, pneumatic artificial muscles (e.g., Muscle Suit [6]), hydraulic actuators, and soft actuators [7].

The current active actuators suffer from being rigid and stiff, which causes them difficulties to adapt to unpredictable impact loads or movement due to their high impedance and resistance. Therefore, the series elastic actuators (SEAs) have been presented as a type of compliant actuator in robotic industries for their various advantages over rigid actuators [8]. The SEA architecture achieves high force control fidelity with low impedance, good bandwidth, and backdriveability. Using feedback force control for SEA, the output force can be measured based on Hooke's law which is related to elastic deformation [9]. Although, the wide use of SEA in different exoskeleton applications, it has been found only a few studies of lumbar support exoskeletons utilized the elastic actuator whether in series or parallel configuration.

The active actuator usually demands a high-power source that may affect the robot's overall mass with limitation of working hours while the passive actuator with its physical nature provides low levels of assistance. In addition, the majority of the current lumbar support exoskeletons have not involved the biomechanical energy conversion of the human movement during the lifting tasks. However, it is still great challenging to achieve a high overall performance of the actuators in the field of

exoskeletons. Therefore, novel energy storage-rotary series elastic actuator (ES-RSEA) has been proposed and developed at the University of Malaya [10] to provide higher torque assistance and compliance with less power consumption in compact and modular design. The key role of ES-RSEA is to harness the kinetic energy through human movement during the lifting task and generate assistance torque without an external power source.

However, the modeling, control design, and dynamic performances have not been investigated for the proposed ES-RSEA. This paper investigates the modeling and dynamic characteristics of the proposed ES-RSEA for lumbar support exoskeleton, and its control architecture is presented. The PID control scheme is designed and analyzed in both torque tracking performance and dynamic characteristics based on the derived dynamic model of the actuator. The sensitivity, compliance, transmissibility, and bandwidth are considered the main criteria for assessing dynamic performance.

2. CONCEPT AND MODELING

A. Actuation Concept Of The ES-RSEA

The classic series elastic actuator (SEA) configuration consists of an output link, spring, transmission reducer, and motor drive, where the attached spring can sense the output torque from its deformation [11]. However, ES-RSEA was modified [12] based on this configuration by combining the spiral spring with an actuator layout. The spiral spring is meant to store and release the energy to provide additional energy to the lumbar support exoskeleton to assist the lifting task. In contrast, the torsional spring operates as the compliant element for the actuator, as shown in the ES-RSEA configuration in Fig. 1.

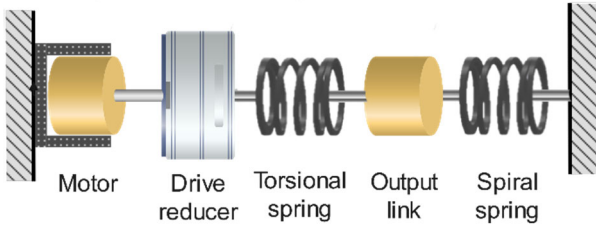


Fig. 1. ES-RSEA configuration

The proposed lumbar support exoskeleton consists of two actuators ES-RSEA located on each hip joint with a flexible wearable structure, as shown in Fig. 3 [12]. ES-RSEA is designed in compact and modular design, as Fig. 2 shows the quarter section view of the actuator. The flat DC brushless motor (EC90, 24 V, 160 W, Maxon motor, Switzerland) was assembled with Harmonic Drive (CSD-25-100-2A-GR, Harmonic Drive®, Germany). The actuator is coupled with two encoders: the MILE encoder (1024 Cpt) is embedded with a DC motor, and the RMB14 angular magnetic encoder (absolute-12 bit-RLS) is set on the axis output link. The planner torsional spring is placed between the harmonic drive and output link while the spiral spring is rigid from one side, and another side is connected to the output link. The design parameters of torsional and spiral springs were optimized based on finite element analysis (FEM) to reduce the weight and size

while maintaining excellent characteristics. Consequently, the stiffness value for the torsional and spiral springs are 450 Nm/rad and 10 Nm/rad, respectively. Also, the maximum output torque is 45.7 Nm with 100 reduction ratios.

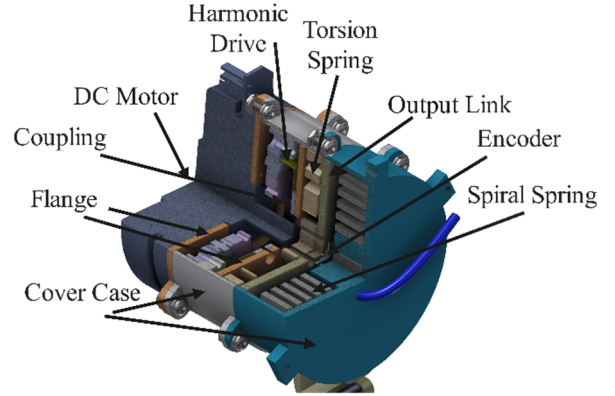


Fig. 2. Quarter-section view of ES-RSEA

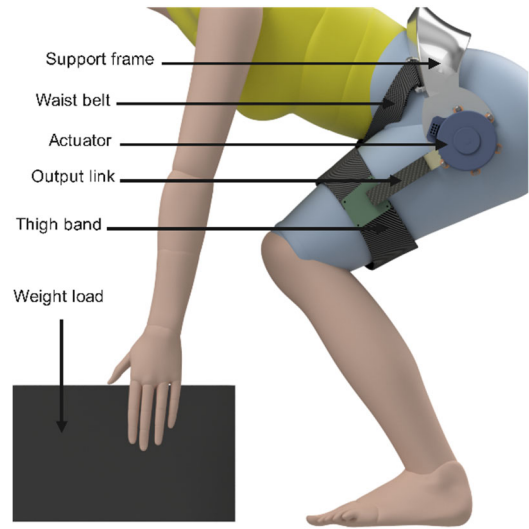


Fig. 3. Soft trunk-hip exoskeleton schematic

B. System Modeling Of The ES-RSEA

a) *Dynamic model*: The actuator ES-RSEA is modeled as a system consisting of rotary elements with a two-mass system and three degrees of freedom, as shown in Fig. 4. The torque output τ_A is proportional to the spring deflection θ_s . By Hooke's law [13], the torque output τ_A of the actuator is:

$$\tau_A = \tau_s - K_2 \theta_1 \quad (1)$$

$$\tau_s = K_1 \theta_s \quad (2)$$

where:

$$\theta_s = (N^{-1} \theta_m - \theta_1) \quad (3)$$

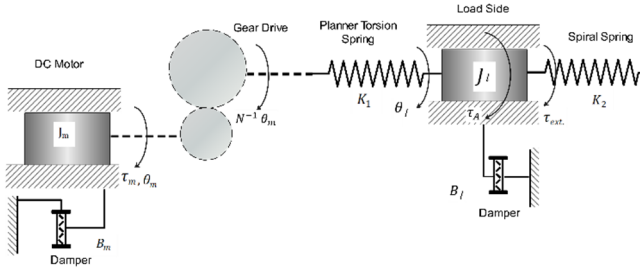


Fig. 4. Schematic diagram of ES-RSEA

Referring to Fig. 4, the equation of motion of the motor side and the load side according to Newton's second law is given by:

$$\tau_m = J_m \ddot{\theta}_m + B_m \dot{\theta}_m + K_1 (N^{-1} \theta_m - \theta_l) N^{-1} \quad (4)$$

$$\tau_{ext} = J_l \ddot{\theta}_l + B_l \dot{\theta}_l + K_1 (\theta_l - N^{-1} \theta_m) + K_2 \theta_l \quad (5)$$

where N is the reduction ratio, τ_a is the assistive torque of the actuator, τ_{ext} is the disturbance torque, τ_m is the generated torque of the motor, J_l is the moment of inertia for the load link, J_m is the moment of inertia of the rotor, B_l is the damping coefficient for the load link, B_m is the damping coefficient of the rotor. K_1 represents the stiffness of torsional spring, K_2 is the stiffness of spiral spring, θ_l is the angle of the load link, θ_m is the output angle of the motor, and θ_s is the spring deformation.

The dynamic model of the proposed ES-RSEA can thus be described in Fig. 5. Note that the dynamic model of the proposed ES-RSEA has different dynamic characteristics compared to the conventional SEA, which is related to the second spring stiffness in the proposed design. The spiral spring is connected to the load side while the other side is fixed. The human factors have not been included in the derived mathematical model since the actuator system is physically interacting with a human joint, and it is not simple to calculate the exact value of the inertia and damping ratio of the human hip joint.

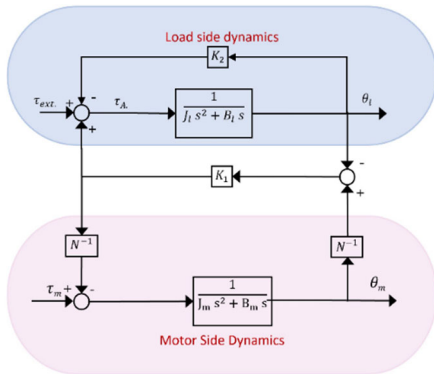


Fig. 5. Block diagram of ES-RSEA

b) Dynamic characteristic analysis: The dynamic analyses were carried out in open-loop and closed-loop analyses to evaluate the actuator characteristics. Based on the open-loop transfer functions, three criteria for assessing the characteristics and performance of ES-RSEA are considered [14], namely force sensitivity, torque transmissibility, and compliance. These transfer functions represent the relationships between the inputs (τ_m the motor torque, and the external torque τ_{ext} .) and

the outputs (three angles θ_l , θ_s and θ_m and the output torque τ_A), as given in Table 1. The variables $P_m(s)$, $P_l(s)$, $D(s)$ and $Q(s)$ shown in Table 1, are defined as:

$$P_m(s) = \frac{1}{J_m s^2 + B_m s} \quad (6)$$

$$P_l(s) = \frac{1}{J_l s^2 + B_l s} \quad (7)$$

$$D(s) = P(s)_1 + P_m(s)N^{-2} + k_1^{-1} \quad (8)$$

$$Q(s) = P_l(s) k_1^{-1} k_2 + P_l(s) P_m(s) N^{-2} k_2 \quad (9)$$

Another dynamic evaluation for the actuator model is the bandwidth analysis of the closed-loop torque control [15]. The block diagram of the bandwidth test is illustrated in Fig. 6. For the bandwidth analysis, it is necessary to fix the output link by setting the input human hip angle (load angle side) to zero. In addition, the saturation function was used in the Simulink model to limit the maximum voltage of the DC motor (24V) for better accurate simulation.

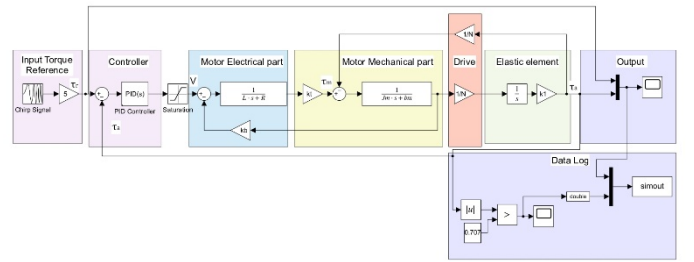


Fig. 6. Block diagram of the bandwidth test

TABLE 1. TRANSFER FUNCTIONS OF ES-RSEA

Criteria	Transfer Function	Proposed ES-RSEA
Transmissibility	$\frac{\tau_A(s)}{\tau_m(s)}$	$\frac{N^{-1} P_m(s)}{D(s) + Q(s)}$
Compliance	$\frac{s \theta_l(s)}{\tau_{ext}(s)}$	$\frac{s P_l(s) (k_1^{-1} + N^{-2} P_m(s))}{D(s) + Q(s)}$
Force Sensitivity	$\frac{\theta_s(s)}{\tau_{ext}(s)}$	$\frac{P_l(s) k_1^{-1}}{D(s) + Q(s)}$

3. TORQUE CONTROL DESIGN

A feedback control loop was implemented to improve the tracking performance of the actuator. A PID controller was implemented to control the ES-RSEA based on the derived dynamic model. For the design of the PID controller, the control scheme was configured, as shown in Fig. 7. The τ_r represents the desired input torque, and the τ_a is the output load torque that would be controlled. The plant is an electromechanical transfer function of ES-RSEA. Since the output torque is estimated depending on the spring deformation, the SEA turns the torque control problem into the spring deformation problem from the motor current decision problem [8]. Moreover, it uses the position encoder as torque feedback. The controller parameters were tuned using the PidTune command in MATLAB with the plant's derived dynamic model. The parameters of the control scheme were identified based on the datasheet of the Maxion DC motor and the physical specification of the dynamic system, as shown in Table 2.

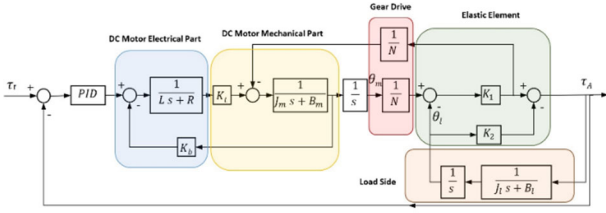


Fig. 7. Control implementation of ES-RSEA

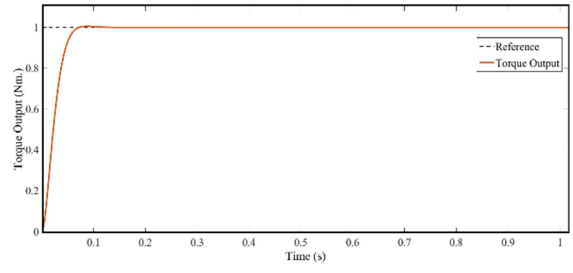


Fig. 9. Torque tracking performance-step reference

TABLE 2. IDENTIFIED PARAMETERS OF ES-RSEA

Parameter	Value
J_l	$1.2578 \times 10^{-4} \text{ kg.m}^2$
B_l	0.08 N.m.s/rad
N	100
J_m	0.0003170 kg.m^2
B_m	0.01 N.m.s/rad ,
K_t	0.0712 Nm/A
K_b	0.0714 rad/s.V
L	0.232 mH
R	0.216Ω

4. RESULTS AND DISCUSSION

A. Torque tracking performance

The dynamic model of actuator ES-RSEA with feedback control loop was commanded to follow the input pattern to validate the torque control performance, which had its frequency 5Hz and amplitude of 1 Nm, with two kinds of torque reference forms, sinusoidal waveform, and step response. The dashed lines in Fig. 8 and Fig. 9 indicate reference signals, and the solid lines represent measured torque outputs. These results indicate that the dynamic model's PID controller can achieve high torque tracking performance up to 5 Hz with a slight phase delay and root-mean-square (RMS) error of 0.1 N.m. There was no overshoot, and the rise time was less than 0.1 sec., which indicates the system's good dynamic performance and response.

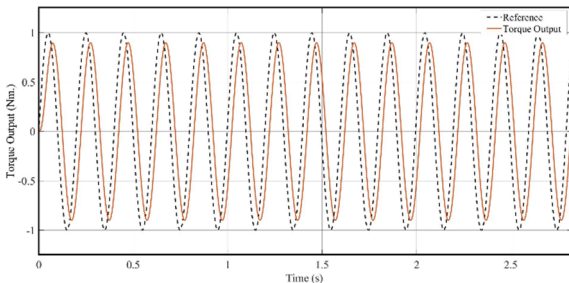


Fig. 8. Torque tracking performance- sinusoidal reference

B. Open-loop transfer function analysis

Three dynamic performances are carried out as evaluation criteria for the actuator based on the open loop-transfer functions for force sensitivity, torque transmissibility, and compliance, as shown in Table 1. The frequency response results are presented as magnitude bode plots using MATLAB.

The force sensitivity result is shown in Fig. 10. The result assures the high magnitude of force sensitivity for the proposed actuator. In other words, the spring can sense the external force and generate spring deformation without affecting the motor side.

The compliance criteria present two different behaviors of the actuator according to frequency range, as shown in Fig. 11. In the low-frequency range, the compliant response increases proportionally with the frequency until it reaches the peak in 2000 rad/s. Then, it drops gradually within the high-frequency range above 2000 rad/s. These compliance attitudes enable the actuator to behave softly at low frequency and rigidly at high-frequency range.

Fig. 12 shows the frequency response results of the transmissibility of the actuator. The results indicate that the transmission ratio of the actuator is nearly steady until the frequency reaches around 40 rad/s. Next, the transmissibility drops gradually to hit the bottom at the frequency of 1000 rad/s; then, it shows a sharp fall after the peak in 2000 rad/s. As a result of decreasing transmissibility at a high-frequency range, the actuator cannot deliver torque from the motor side to output within these frequencies. However, the actuator design requirement of the lumbar support exoskeleton does not require a high frequency to operate the lifting tasks. Therefore, the torque transmissibility of the actuator is good at the low-frequency range as desired for the application.

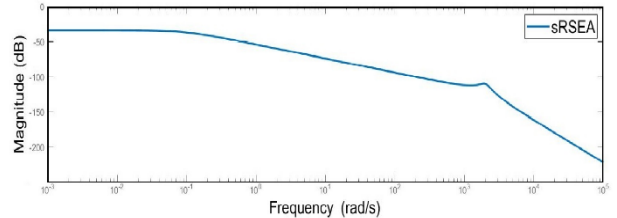


Fig. 10. Frequency response of force sensitivity

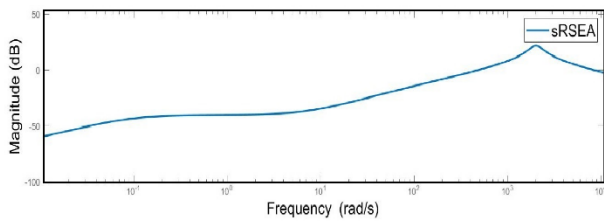


Fig. 11. Frequency response of compliance

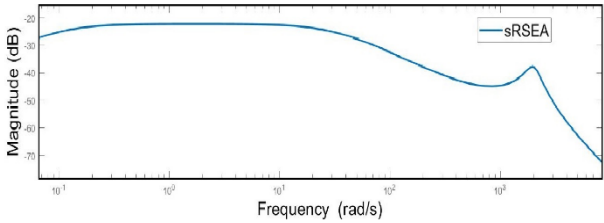


Fig. 12. Frequency response of transmissibility.

C. Close-loop analysis

To benchmark, the proposed actuation's versatility and torque control bandwidth for the closed-loop system is used as a metric to demonstrate the actuator's overall performance and validate whether the proposed design meets the bandwidth requirement of hip joint movement. The input reference torque was commended by implementing the sinusoidal chirp signal with a range from 0 to 100 Hz and a magnitude of 45 Nm, as shown in Fig. 6. The simulation result was carried out as a Bode plot, as illustrated in Fig. 13. The Bode plot shows that the actuator model reaches high bandwidth of 12.44 Hz. The bandwidth simulation may contrast with the experiment and actual results due to the model's simplicity and assumptions. However, the bandwidth simulation analysis can assure the actuator model's underlying characteristics with the system bandwidth (12.44 Hz). Compared with the Back-Support Exoskeleton (Mk2) [16] utilizing PEA with 4.85 Hz bandwidth, the bandwidth control of ES-RSEA is more robust and safer with uncertainties.

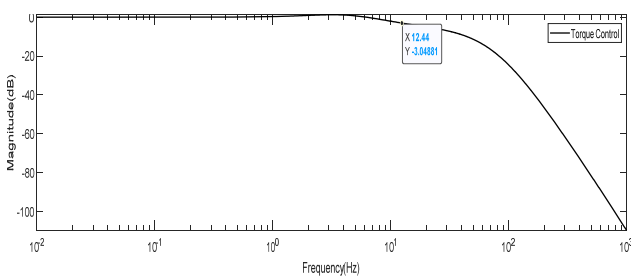


Fig. 13. Bandwidth result

5. CONCLUSION AND FUTURE WORK

This paper proposes the mathematical model and control design of a novel ES-RSEA for the lumbar support exoskeleton, and its dynamic characteristic is investigated. The ES-RSEA exploits the biomechanics of lifting movement to store the kinetic energy and then release the energy as additional assistance torque. The frequency response analysis of this actuation paradigm exhibits high force sensitivity and high compliance at low frequency. It can deliver torque to the load side with good transmissibility at the low-frequency and fulfill the hip

joint's required frequency with a high bandwidth (12.44 Hz) without implementing complicated control methods. The torque tracking analysis shows that the PID controller of the actuator could track the input command with an approximate root-mean-square (RMS) torque error of 0.1 Nm and no overshoot. Consequently, ES-RSEA has the potential to ensure compliance and high response to handle unexpected human movements, preventing any injury and reducing exoskeleton structure and motor damage.

The limitation of this study is that there is no experiment study to implement a control scheme into the actual hardware test for the ES-RSEA. The proposed torque controller is not optimal yet. Our future work will investigate the adaptive control strategies using this experiment platform and assess the dynamics characteristics of the actuator.

ACKNOWLEDGMENT

The authors wish to acknowledge the support by the University of Malaya for the facility and equipment support under the faculty of engineering Grant (GPF023A-2018).

REFERENCES

- [1] P. Brinckmann et al., "Quantification of overload injuries to thoracolumbar vertebrae and discs in persons exposed to heavy physical exertions or vibration at the work-place: The shape of vertebrae and intervertebral discs — study of a young, healthy population and a middle-aged control group," *Clinical Biomechanics*, vol. 9, pp. S3-S83, 1994/01/01/ 1994, doi: [https://doi.org/10.1016/0268-0033\(94\)90074-4](https://doi.org/10.1016/0268-0033(94)90074-4).
- [2] H. Kazerooni, "Human power amplifier for lifting load including apparatus for preventing slack in lifting cable," US Patent Appl. pct/us00/04065, 2000. [Online]. Available: <https://patents.google.com/patent/WO2000069771A1/nl>
- [3] Z. Yang, W. Gu, J. Zhang, and L. Gui, *Force control theory and method of human load carrying exoskeleton suit*. Springer, 2017.
- [4] A. J. Young and D. P. Ferris, "State of the Art and Future Directions for Lower Limb Robotic Exoskeletons," *IEEE Trans Neural Syst Rehabil Eng*, vol. 25, no. 2, pp. 171-182, Feb 2017, doi: 10.1109/TNSRE.2016.2521160.
- [5] X. Ji et al., "SIAT-WEXv2: A Wearable Exoskeleton for Reducing Lumbar Load during Lifting Tasks," *Complexity*, vol. 2020, pp. 1-12, 2020/11/28 2020, doi: 10.1155/2020/8849427.
- [6] T. Ito, K. Ayusawa, E. Yoshida, and H. Kobayashi, "Stationary torque replacement for evaluation of active assistive devices using humanoid," in 2016 IEEE-RAS 16th International Conference on Humanoid Robots (Humanoids), 15-17 Nov. 2016 2016, pp. 739-744, doi: 10.1109/HUMANOIDS.2016.7803356. [Online]. Available: <https://ieeexplore.ieee.org/ielx7/7786013/7803244/07803356.pdf?tp=&arnumber=7803356&isnumber=7803244&ref=>
- [7] R. A. R. C. Gopura, K. Kiguchi, and D. S. V. Bandara, "A brief review on upper extremity robotic exoskeleton systems," in 2011 6th International Conference on Industrial and Information Systems, 16-19 Aug. 2011 2011, pp. 346-351, doi: 10.1109/ICIINFS.2011.6038092.
- [8] G. A. Pratt and M. M. Williamson, "Series elastic actuators," in Proceedings 1995 IEEE/RSJ International Conference on Intelligent Robots and Systems. Human Robot Interaction and Cooperative Robots, 1995, vol. 1, pp. 399-406 vol.1, doi: 10.1109/IROS.1995.525827. [Online]. Available: <https://ieeexplore.ieee.org/document/525827/>
- [9] J. Pratt and B. T. Krupp, *Series Elastic Actuators for legged robots*. 2004.
- [10] O. S. Al-Dahiree, R. A. R. Ghazilla, M. O. Tokhi, H. J. Yap, and E. A. Albaadani, "Design of a Compact Energy Storage with Rotary Series Elastic Actuator for Lumbar Support Exoskeleton," *Machines*, vol. 10, no. 7, 2022 2022, doi: 10.3390/machines10070584.

- [11] D. W. Robinson, J. E. Pratt, D. J. Paluska, and G. A. Pratt, "Series elastic actuator development for a biomimetic walking robot," in 1999 IEEE/ASME International Conference on Advanced Intelligent Mechatronics (Cat. No.99TH8399), 19-23 Sept. 1999 1999, pp. 561-568, doi: 10.1109/AIM.1999.803231. [Online]. Available: <https://ieeexplore.ieee.org/document/803231/>
- [12] O. S. Al-Dahiree, R. A. R. Ghazilla, M. O. Tokhi, H. J. Yap, and E. A. Albaadani, "Design of a Compact Energy Storage with Rotary Series Elastic Actuator for Lumbar Support Exoskeleton," *Machines*, vol. 10, no. 7, p. 584, 2022. [Online]. Available: <https://www.mdpi.com/2075-1702/10/7/584>.
- [13] B. Hu, G. Cheng, H. Lu, and H. Yu, "Optimal Design of the Elastic Unit for the Serial Elastic Hip Joint of the Lower Extremity Exoskeleton," in *Man-Machine-Environment System Engineering*, Singapore, S. Long and B. S. Dhillon, Eds., 2020// 2020: Springer Singapore, pp. 85-94.
- [14] C. Lee, S. Kwak, J. Kwak, and S. Oh, "Generalization of Series Elastic Actuator Configurations and Dynamic Behavior Comparison," *Actuators*, vol. 6, no. 3, p. 26, 2017. [Online]. Available: <https://www.mdpi.com/2076-0825/6/3/26>.
- [15] S. Yu et al., "Quasi-Direct Drive Actuation for a Lightweight Hip Exoskeleton With High Backdrivability and High Bandwidth," *IEEE/ASME Transactions on Mechatronics*, vol. 25, no. 4, pp. 1794-1802, 2020, doi: 10.1109/TMECH.2020.2995134.
- [16] S. Toxiri, A. Calanca, J. Ortiz, P. Fiorini, and D. G. Caldwell, "A Parallel-Elastic Actuator for a Torque-Controlled Back-Support Exoskeleton," *IEEE Robotics and Automation Letters*, vol. 3, no. 1, pp. 492-499, 2018, doi: 10.1109/LRA.2017.2768120.